

# Sliding-Mode Control of a Permanent-Magnet Synchronous Motor with Uncertainty Estimation

Markus Reichhartinger and Martin Horn

*Abstract*—In this paper, the application of sliding-mode control to a permanent-magnet synchronous motor (PMSM) is presented. The control design is based on a generic mathematical model of the motor. Some dynamics of the motor and of the power amplification stage remain unmodelled. This model uncertainty is estimated in realtime. The estimation is based on the differentiation of measured signals using the ideas of robust exact differentiator (RED). The control law is implemented on an industrial servo drive. Simulations and experimental results are presented and compared to the same control strategy without uncertainty estimation. It turns out that the proposed concept is superior to the same control strategy without uncertainty estimation especially in the case of non-smooth reference signals.

*Keywords*—sliding-mode control, Permanent-magnet synchronous motor, uncertainty estimation, robust exact differentiator.

## I. INTRODUCTION

**P**ERMANENT-magnet synchronous motors (PMSMs) nowadays are commonly used in industrial applications in the field of motion control. Major reasons for their popularity are high power density and high efficiency. PMSMs belong to the class of AC motors for which a number of advanced control techniques have been developed in the recent years [1]–[5].

In this paper, the field oriented control (FOC) method [6] in an industrial servo drive is considered. It is based on the so-called  $(d, q)$ -coordinate frame which is fixed with respect to the rotor position. The popularity of PMSMs in combination with FOC is documented by numerous publications, e.g. [7], [8]. Usually the FOC approach is implemented in cascaded feedback loops. The inner loop is dedicated to control the motor currents. According to the application outer loops for speed or position control are added.

This work deals with the current control loop design which is based on a commonly used PMSM model. In contrast to popular approaches the proposed control law accounts for unmodelled uncertainties mainly introduced by the power amplification stage.

The paper is organized as follows: In Section II a dynamic model of the PMSM and the proposed control strategy are presented. Section II-C describes the differentiation scheme used for uncertainty estimation. Numerical simulations to find initial controller parameters are presented in Section III. The experimental setup and the results are explained and illustrated in Section IV. Section V concludes this paper.

M. Reichhartinger and M. Horn are with the Institute of Smart System-Technologies, Control- and Measurement Systems Group, Klagenfurt University, Klagenfurt, Austria, e-mail: markus.reichhartinger@uni-klu.ac.at.

## II. CONTROL

### A. Plant Model

The mathematical model describing the electrical part of a PMSM is given by

$$\frac{di_d}{dt} = -\frac{R}{L}i_d + \omega_e i_q + \frac{1}{L}u_d, \quad (1a)$$

$$\frac{di_q}{dt} = -\frac{R}{L}i_q - \omega_e i_d - \frac{1}{L}\lambda\omega_e + \frac{1}{L}u_q, \quad (1b)$$

where the motor parameters  $R$ ,  $L$  and  $\lambda$  are the winding resistance, the winding inductance and the flux linkage respectively [9]. The electrical angular velocity  $w_e$  is computed with the help of the measured mechanical velocity  $\omega_m$  and the number  $z_p$  of pole pairs via

$$w_e = z_p \omega_m. \quad (2)$$

The currents  $i_d$  and  $i_q$  represent the measured phase currents after applying the required transformations [2]. The voltages  $u_d$  and  $u_q$  are the control signals, which have to be retransformed into the phase coordinate frame. As usual it is assumed that  $i_d$  is steered to zero with the help of an existing PI-controller. Therefore it suffices to stick to differential equation (1b), which describes the dynamic behaviour of the torque-generating current  $i_q$ . This model has been used as basis for the controller design in many applications, e.g. [7], [9], [10]. Nevertheless it does not take into account effects like the nonlinear behaviour of the inductance  $L$  and the flux linkage  $\lambda$ . Effects introduced by the power amplification stage are neglected as well. In order to account for the above mentioned phenomena an additional term  $\Delta$ , representing the model uncertainty is introduced. This yields the extended plant model

$$\frac{di_q}{dt} = -\frac{R}{L}i_q - \omega_e i_d - \frac{1}{L}\lambda\omega_e + \frac{1}{L}u_q + \Delta, \quad (3)$$

where  $\Delta$  is assumed to be bounded.

### B. Controller Design

The smooth reference signal  $r$  for the  $i_q$  component is either a given desired torque or a signal generated from the outer cascade layer. The goal of the controller is to drive the control error

$$x_1 := i_q - r \quad (4)$$

to zero asymptotically. In order to guarantee vanishing steady state error, the state variable  $x_0$  is introduced as the integral of the control error  $x_1$ , so that the design model takes the form

$$\frac{dx_0}{dt} = x_1 \quad (5a)$$

$$\frac{dx_1}{dt} = -\frac{R}{L}(x_1 + r) - \omega_e i_d - \frac{1}{L}\lambda\omega_e + \frac{1}{L}u_q - \frac{dr}{dt} + \Delta. \quad (5b)$$

A standard sliding-mode control law, based on the linear sliding surface

$$\sigma := x_1 + \gamma x_0 \quad \text{with } \gamma > 0, \quad (6)$$

and satisfying the  $\eta$  reaching condition [11]

$$\text{sign}(\sigma) \frac{d\sigma}{dt} \leq -\eta \quad \text{with } \eta > 0 \quad (7)$$

is given by

$$u_q = R(x_1 + r) + L\omega_e i_d + \lambda\omega_e + L \frac{dr}{dt} - L\gamma x_1 - L\Delta_{est} - \eta L \text{sign}(\sigma), \quad (8)$$

where  $\Delta_{est}$  is the estimated uncertainty, see below. In order to reduce chattering a boundary layer around  $\sigma = 0$  is introduced by replacing the  $\text{sign}$ -function by a saturation function, i.e.

$$\text{sign}(\sigma) \rightarrow \text{sat}(\sigma/\Phi), \quad (9)$$

where the positive constant  $\Phi$  is the boundary layer thickness [12], [13].

### C. Uncertainty Estimation

The uncertainty estimation is based on the rearranged equation (3), i.e.

$$\Delta_{est} = \frac{R}{L}i_q + \omega_e i_d + \frac{1}{L}\lambda\omega_e - \frac{1}{L}u_q + \left. \frac{di_q}{dt} \right|_{est}, \quad (10)$$

where  $\left. \frac{di_q}{dt} \right|_{est}$  is the estimated value of  $\frac{di_q}{dt}$ . The differentiation of  $i_q$  with respect to time is realized on ideas of robust exact differentiation as proposed in [14] and successfully demonstrated in numerous applications, e.g. [15]–[17]. Of course alternative differentiation schemes, e.g. algebraic methods as outlined in [18] and realized in [19] can be employed instead. In the present case the output  $\hat{i}_q$  of an integrator has to track the measured current  $i_q$ . Therefore the time-derivative of  $\hat{i}_q$  can be regarded as the estimate for  $\frac{di_q}{dt}$ , i.e.

$$\left. \frac{di_q}{dt} \right|_{est} = \frac{d\hat{i}_q}{dt}. \quad (11)$$

Tracking is ensured by the so-called super twisting algorithm as outlined in [20], [21]

$$\frac{d\zeta}{dt} = -\kappa \text{sign}(\epsilon), \quad (12)$$

$$\left. \frac{di_q}{dt} \right|_{est} = \zeta - \theta \sqrt{|\epsilon|} \text{sign}(\epsilon), \quad (13)$$

where the error

$$\epsilon := \hat{i}_q - i_q \quad (14)$$

vanishes in finite time. The parameters  $\kappa$  and  $\theta$  are strictly positive constants which have to be chosen according to [14].

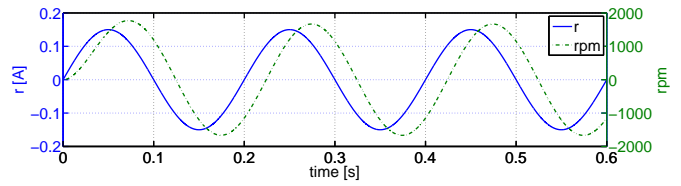


Fig. 1. Result of simulation with initial parameters for experiment.

## III. SIMULATION

Initial controller parameters are found by numerical simulation. In simulation the nominal model (1a), (1b) represents the plant. Hence the control law is implemented without uncertainty estimation II-C. The PI-controller, which steers the current  $i_d$  to zero uses prescribed controller parameters, see section IV-A. The model is extended by a differential equation describing the rotor's motion including viscous friction.

### A. Controller Tuning

For the motor under consideration it is known that a voltage  $u_q \approx 30V$  is required to adjust the nominal value of  $|i_q|_{max} = 0.5A$ . This a priori knowledge is used to determine the initial weight  $\eta$  of the discontinuous control component, i.e.

$$\eta L \approx 30V \rightarrow \eta \approx \frac{30}{L} = \frac{30}{20 \cdot 10^{-3}} = 1500. \quad (15)$$

It should be noted that this estimate is very crude and just is used to find initial settings. The parameter  $\gamma$  and the boundary layer thickness  $\Phi$  are initially chosen sufficiently small, i.e.

$$\gamma \ll 1 \quad \text{and} \quad \Phi \ll 1.$$

Based on simulations results both parameters were increased iteratively in order to improve the tracking performance.

### B. Differentiator tuning

The overall concept requires the implementation of two differentiators. Both were realized as REDs as outlined in section II-C. While the parameter tuning of the RED applied to the noise free reference signal  $r$  is straight forward, the tuning of the differentiator for computing  $\left. \frac{di_q}{dt} \right|_{est}$  requires remarkable effort. Measurements of the current  $i_q$  taken from experiments without uncertainty estimation are used to tune the RED parameters  $\kappa$  and  $\theta$  offline.

### C. Results

The final setting used for a first real world experiment is summarized in Table I. Exemplarily a simulation result is illustrated in Figure 1. The sinusoid reference signal  $r$  has an amplitude  $r_{max} = 0.15A$  and a frequency of  $5Hz$ . The absolute value of the control error  $x_1$  does not exceed a bound of  $5 \cdot 10^{-3}A$ . The dashed green curve in Figure 1 shows the expected motor-shaft speed.

TABLE I  
 INITIAL CONTROL PARAMETERS GAINED BY SIMULATION

CONTROLLER		RED: $r$	
Parameter	Value	Parameter	Value
$\gamma$	1000	$\theta$	10
$\Phi$	0.15	$\kappa$	5
$\eta$	1500		

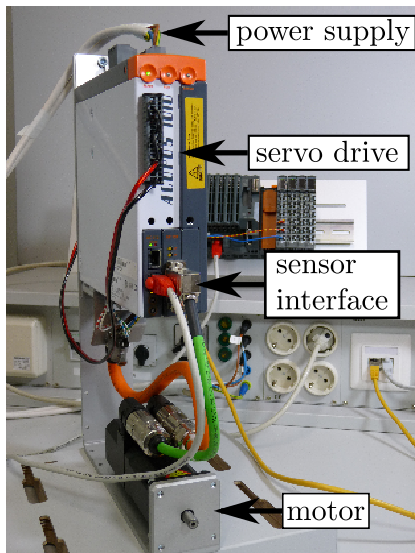


Fig. 2. Foto of the experimental setup [22].

#### IV. EXPERIMENT

##### A. Experimental Setup

The control law is implemented on a digital signal processor (DSP) in an industrial servo drive which is depicted in Figure 2. The control law is part of the operating system, i.e. changes to the control law require a complete recompilation of the operating system. The motor parameters are summarized in Table II. The currents are sampled with a sampling period of  $6.25\mu s$  using 14-bit analog to digital converters. The arithmetic mean value of the last eight samples is used in the control law, which is executed with a sampling period of

$$T_s = 50\mu s. \quad (16)$$

The control signals  $u_q$  and  $u_d$  are transformed into corresponding pulse width modulated phase voltages. The switching frequency of the power stage is  $20kHz$ .

##### B. Results

The final controller setting and the parameters for the REDs used to differentiate the reference signal  $r$  and the current

TABLE II  
 MOTOR PARAMETERS

Parameter	Value	Unit
$R$	50	$\Omega$
$L$	0.02	$H$
$\lambda$	1.7	$Vs$

TABLE III  
 CONTROL PARAMETERS

CONTROLLER		RED: $r$		RED: $i_q$	
Parameter	Value	Parameter	Value	Parameter	Value
$\gamma$	200	$\theta$	75	$\theta$	5
$\Phi$	0.15	$\kappa$	2	$\kappa$	0.5
$\eta$	800				

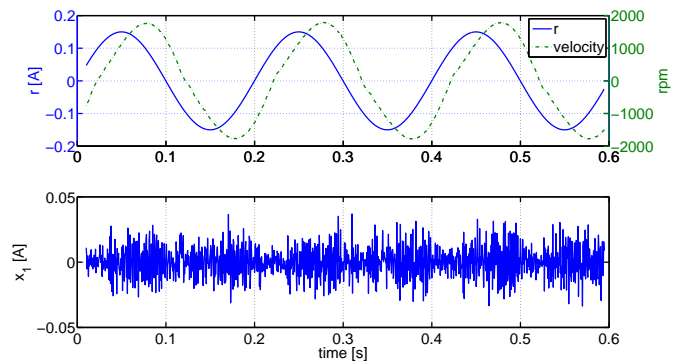


Fig. 3. Experiment with uncertainty estimation

$i_q$  are listed in Table III. The controller parameters with uncertainty estimation yield good performance, the maximum absolute value of the tracking error  $x_1$  remains below  $0.05A$ , see Figure 3. Friction effects are noticeable especially for low motor speeds. Experiments reveal that the uncertainty estimation in non-nominal operating points improves the tracking performance. Figure 4 shows the control signal  $u_q$  and its estimated uncertain component  $L \Delta_{est}$ , compare equation (8). The maximum absolute value of the voltage due to uncertainty estimation is  $17V$ , which is approximately 20 percent of the control signal  $u_q$ .

The same experiment was carried out *without* uncertainty estimation, see Figure 5. It can be seen that the tracking performance deteriorates, especially at high accelerations and for alternating directions of rotation. The proposed control strategy with parameter estimation is also able to cope with non-smooth reference signals. Results of an experiment with a rectangular reference signal are presented in Figure 6. The amplitude of  $r$  is  $0.3A$ , the frequency is chosen such that the velocity of the motor is higher than the nominal revolution speed of 6000 rpm. It is worth to be mentioned that the control law without uncertainty estimation is not able to track the non-smooth reference signal with the controller setting listed in Table III.

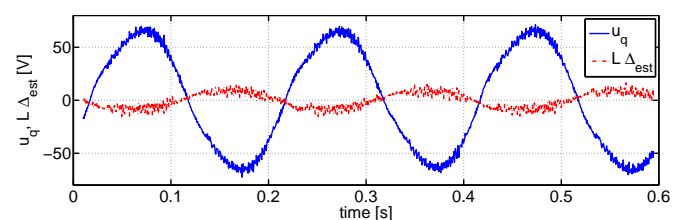


Fig. 4. Voltages  $u_q$  and  $L \Delta_{est}$

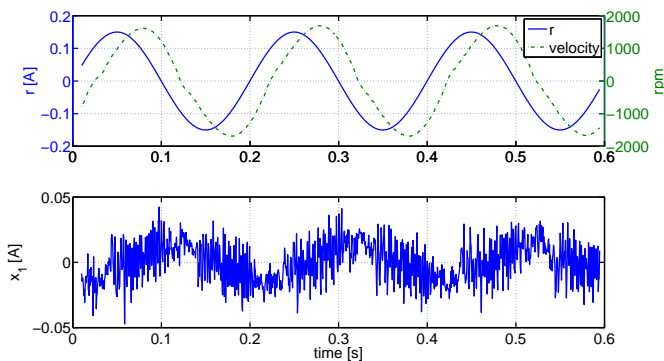


Fig. 5. Experiment without uncertainty estimation

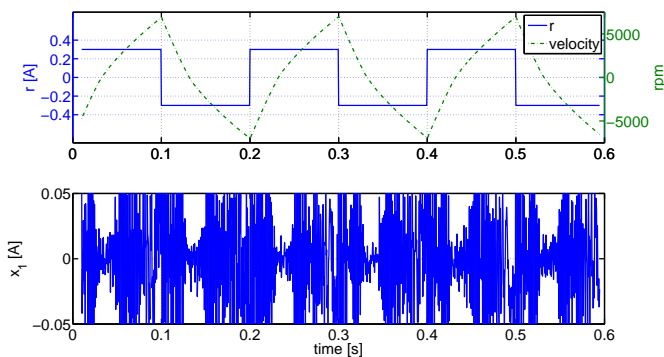


Fig. 6. Experiment with uncertainty estimation and non-smooth reference signal  $r$

## V. CONCLUSION

An integrating sliding-mode control law is implemented on an industrial servo drive. A generic mathematical model is used to describe the dynamics of the motor, the power amplification stage and some nonlinear effects remain unmodelled. An additional term representing bounded uncertainties is introduced. The control law using the estimated uncertainty by means of the RED is realized on a DSP. Numerical simulations provide control parameters for practical experiments. Real world experiments are discussed in order to illustrate the effectiveness of the proposed method.

## ACKNOWLEDGMENT

This work was kindly supported by Bernecker & Rainer Industrie-Elektronik Ges.m.b.H., Eggelsberg, Austria [22]. Special thanks to Dipl.-Ing. Roland Reichhartinger for his help and his valuable contributions to this work.

## REFERENCES

- [1] J. A. Santisteban and R. M. Stephan, "Vector control methods for induction machines: an overview," *IEEE Transactions on Education*, vol. 44, no. 2, pp. 170–175, May 2001.
- [2] R. Krishnan, *Electric Motor Drives, Modeling, Analysis, and Control*. Prentice Hall, Inc., 2001.
- [3] R.-M. Jan, C.-S. Tseng, and R.-J. Liu, "Robust pid control design for permanent magnet synchronous motor: A genetic approach," *Electric Power Systems Research*, vol. 78, no. 7, pp. 1161 – 1168, 2008.

- [4] Z. Song, Z. Hou, C. Jiang, and X. Wei, "Sensorless control of surface permanent magnet synchronous motor using a new method," *Energy Conversion and Management*, vol. 47, no. 15-16, pp. 2451 – 2460, 2006.
- [5] Q. Jilong, T. Yantao, G. Yimin, and Zhucheng, "A sensorless initial rotor position estimation scheme and an extended kalman filter observer for the direct torque controlled permanent magnet synchronous motor drive," in *Proc. International Conference on Electrical Machines and Systems ICEMS 2008*, 17–20 Oct. 2008, pp. 3945–3950.
- [6] F. Blaschke, "The principles of field orientation as applied to the new transvektor closed-loop control system for rotating field machines," *Siemens Review*, pp. pp. 217–220, 1972.
- [7] K. Song, W. Liu, and G. Luo, "Permanent magnet synchronous motor field oriented control and hil simulation," in *Proc. IEEE Vehicle Power and Propulsion Conference VPPC '08*, 3–5 Sept. 2008, pp. 1–6.
- [8] A. Cavallo and C. Natale, "Second order sliding output control of permanent magnet synchronous machines," *IEEE Conference on Decision and Control*, vol. 48, 2009.
- [9] V. Utkin, J. Guldner, and J. Shi, *Sliding Mode Control in Electromechanical Systems*. Taylor and Francis Ltd, 1999.
- [10] J. Simanek, J. Novak, O. Cerny, and R. Dolecek, "Foc and flux weakening for traction drive with permanent magnet synchronous motor," in *Proc. IEEE International Symposium on Industrial Electronics ISIE 2008*, June 30 2008–July 2 2008, pp. 753–758.
- [11] C. Edwards and S. K. Spurgeon, *Sliding Mode Control, Theory and Applications*. Taylor and Francis Ltd, 1998.
- [12] V. I. Utkin, *Sliding Modes in Control and Optimization*. Springer, 1992.
- [13] J. Slotine and W. Li, *Applied Nonlinear Control*. Prentice Hall, 1991.
- [14] A. Levant, "Higher-order sliding modes, differentiation and output-feedback control," *International Journal of Control*, vol. 76, pp. 924–941, 2003.
- [15] M. Reichhartinger and M. Horn, "Application of higher order sliding-mode concepts to a throttle actuator for gasoline engines," *IEEE Transactions on Industrial Electronics*, vol. 56, no. 9, pp. 3322–3329, Sept. 2009.
- [16] F. Robles-Aguirre, J. Canedo, L. Fridman, and A. Loukianov, "Second order sm unified power flow controller for power systems," in *Proc. International Workshop on Variable Structure Systems VSS '08*, 2008, pp. 349–354.
- [17] A. Colbia-Vega, J. de Leon-Morales, L. Fridman, O. Salas-Pena, and M. Mata-Jimenez, "Robust excitation control design using sliding-mode technique for multimachine power systems," *Electric Power Systems Research*, vol. 78, pp. 1627–1634, September 2008.
- [18] M. Fliess, C. Join, and H. Sira Ramirez, "Non-linear estimation is easy," *Int. J. Modelling, Identification and Control*, vol. 4, no. 1, pp. 12–27, 2008.
- [19] J. Zehetner, J. Reger, and M. Horn, "A derivative estimation toolbox based on algebraic methods - theory and practice," in *Proceedings of the IEEE Conference on Control Applications*, 2007, pp. pp. 331–336.
- [20] A. Levant, "Robust exact differentiation via sliding mode technique," *automatica*, vol. 34, no. 3, pp. 379–384, 1998.
- [21] —, "Principles of 2-sliding mode design," *automatica*, vol. 43, pp. 576–586, April 2007.
- [22] Bernecker + Rainer Industrie-Elektronik Ges.m.b.H. [Online]. Available: <http://www.br-automation.com/>